Differences between Seasonal and Mean Annual Energy Balance Model Calculations of Climate and Climate Sensitivity

GERALD R. NORTH[1]

Department of Physics, University of Missouri, St. Louis 63121

JAMES A. COAKLEY, JR.

National Center for Atmospheric Research[2], Boulder, CO 80307

(Manuscript received 27 September 1978, in final form 6 March 1979)

ABSTRACT

A simple Budyko-Sellers mean annual energy balance climate model with diffusive transport (North, 1975b) is extended to include a seasonal cycle. In the model the latitudinal distribution of the zonal average surface temperature is represented by a series of Legendre polynomials, while its time-dependence is represented by a Fourier sine-cosine series. The model has three parameters which are adjusted so that the observed amplitudes of the Northern Hemisphere's zonal mean surface temperature are recovered. In order to obtain the correct amplitude and phase of the surface temperature's seasonal oscillation, allowance must be made for the disparity between the thermal inertia of the atmosphere over continents and that of the ocean's mixed layer. Although the model parameters are adjusted to recover the surface temperature fields of the Northern Hemisphere, a test of the model's ability to produce the fields of the Southern Hemisphere indicates that the model responds properly to changes in boundary conditions.

The seasonal model is used to reveal how the annual mean climate and its sensitivity to changes in incident radiation differ from the predictions obtained with the corresponding mean annual model. Although the zonal temperatures obtained with the seasonal model are 1–3°C higher than those obtained with the mean annual model, the changes in the global average annual mean surface temperatures calculated with the two models are practically identical for a 1% decrease in solar constant. Furthermore, because the albedo changes in them are linked mainly to changes in surface temperature, both models respond in the same manner to changes in the incident solar radiation caused by changes in the earth's orbit. The distribution of the incident solar radiation in the models is shown to be insensitive to changes in the eccentricity and the longitude of perihelion and sensitive only to changes in the obliquity of the earth. For past orbital changes, both the seasonal and the mean annual model fail to produce glacial advances of the magnitude that are thought to have occurred.

1. Introduction

The recent interest in simple heat-balance climate models is due mainly to Budyko (1969) and Sellers (1969) who independently showed that the sensitivity of the climate might be greatly enhanced by the temperature-albedo feedback mechanism. In fact, both authors pointed out that, according to their models, if the solar constant were lowered by only a few percent, a transition would be made to an ice-covered planet. The possibility of such extreme sensitivity to external controls and similarly to internal parameters possibly influenced by man's activities has led to a large research effort directed toward understanding the planetary climate. A part of this effort has been the study of climate and climate change with a hierarchy of models, the Budyko-Sellers versions being among the simplest members of the hierarchy and global circulation models (GCM) being the most complicated. The advantages gained by using a spectrum of models are obvious—physical interpretation and solubility of simple models and closeness to reality of the large models. The philosophy of such an approach has been reviewed by Schneider and Dickinson (1974).

The Budyko-Sellers models are highly parameterized. The terms which enter the heat-balance equation have simple mathematical forms so that solutions to the model are readily obtained. The models originally described by Budyko and Sellers were zonally and seasonally averaged. They pertained only to annual mean conditions. The purpose of this paper is to relax the latter limitation so that the seasonal cycle is included.

[1] Present affiliation: Goddard Laboratory for Atmospheric Sciences, Goddard Space Flight Center, NASA, Greenbelt, MD 20771.

[2] The National Center for Atmospheric Research is sponsored by the National Science Foundation.

0022-4928/79/071189-16$08.00

The reason for such an extension is to see how the seasonal oscillation can be simulated with a minimum of free parameters. We hope to reveal the leading mechanisms in the large-scale march of the seasons; how the mean annual climate is affected by seasonal residuals, such as the correlation between albedo and incident solar radiation at high latitudes, and how the sensitivity of the seasonal model differs from that calculated with the mean annual model.

Seasonal models have been developed by a number of authors, including Adem (1962), Wetherald and Manabe (1972), Sellers (1973, 1976) and Suarez and Held (1976). Our model is more modest in that the physical mechanisms included in it are idealized. In its way, however, our model is rigorous in that the number of adjustable parameters is small and these parameters are always explicit. We believe that this study is useful as a guide for further experimentation with more realistic models and because it clearly isolates various causal relationships.

In this paper we will adopt a philosophy previously discussed by one of us (North, 1975b): simple models can be expected to work on time scales that are long compared with the time scales of weather fluctuations and on spatial scales that are large compared with the spatial scales of weather systems. As one begins to ask questions about smaller space or time scales the simple heat-balance model must fail because it neglects many physical processes, mean motions, etc., which affect the small-scale structure of the system. On the other hand, by taking averages over large distances and long time periods, one gains the advantages of adding together information that is statistically uncorrelated and therefore similar to an ensemble average. It is in this spirit, for example, that the zonally averaged heat divergence is modeled by diffusion. Of course, the principle suggested here has no rigorous proof and is admittedly an optimistic conjecture.

Since at best the model is appropriate to large spatial scales and long time scales, it is advantageous to adopt from the beginning a solution procedure which starts with the largest and slowest scales and adds on as corrections the finer scale information. Fortunately, this separation of the large spatial and slow time scales is easy to do with heat-balance models, and it has been done in some earlier studies (Fritz, 1960; Held and Suarez, 1974; North, 1975a,b). If diffusion is the transport mechanism, and if the flux of infrared radiation emitted is linear in the surface temperature (Budyko, 1969; Cess, 1976), Legendre polynomials form a natural basis set. Because they diagonalize the diffusion operator, the mode amplitudes of the Legendre polynomials satisfy algebraic equations which are uncoupled. Similarly, in the time variable, the appropriate basis functions are sines and cosines with succeeding terms representing mean annual, annual harmonic, semiannual harmonic, etc.

It has been suggested that the gross features of the mean annual climate can be represented by a Fourier-Legendre series including contributions from only the $P_0(x)$ and $P_2(x)$ terms (North, 1975b). In this paper we extend this treatment by adding a north-south asymmetric $P_1(x)$ term whose coefficient is first harmonic in time. An effort along these lines was made years ago by Fritz (1960), but it was done without the benefit of the parameterizations introduced by Budyko and Sellers and the recent satellite data which have been analyzed by Ellis and Vonder Haar (1976).

Since the extent of ice caps predicted with mean annual models has proven to be rather insensitive to changes in the earth's orbital parameters (Sellers, 1970; Budyko, 1969; Saltzman and Vernekar, 1971; Coakley, 1979), it has often been conjectured that the periodic glaciation of the earth must be influenced by the seasonal cycle (Budyko, 1969; Kukla and Kukla, 1974). Hence, one motivation for constructing a seasonal model is to check this hypothesis. Therefore, we shall attempt to do this within the confines of simple heat-balance schemes.

Our treatment begins by showing that the seasonal zonally averaged fields of temperature, infrared radiation and albedo may be represented satisfactorily by only a few terms in the proposed series of basis functions. The convergence is best when the data are symmetrized so that the Northern and Southern Hemispheres are made to appear identical. In Section 3 it is shown that the distribution of incident solar radiation may also be satisfactorily represented by only a few terms in the series. Since the driving terms and responses are simply represented with an obviously diagonal transfer matrix, we can easily generalize the mean annual model to include a seasonal cycle. Such a model is constructed for the Northern Hemisphere in Section 4 with examples given in Section 5. The model is then tested in Section 6 by application to what amounts to a different planet—the symmetrized Southern Hemisphere. In Section 7 the seasonal model climate is compared to the mean annual model climate. After a suitable albedo parameterization is adopted in Section 8, it is possible to test the sensitivity of the model to changes in the solar constant in order to compare the sensitivity with that of the mean annual model. Section 9 contains the calculations of climatic change caused by changes in the earth's orbital parameters. Conclusions are presented in Section 10.

2. Seasonal data

Zonally averaged fields of climatic interest such as surface temperature, albedo, etc., are usually presented in tables of month-long averages for var-

ious latitude belts. For modeling these fields, however, it is more convenient to use their Fourier time series since, in some cases, we may gain physical insight from the relative sizes of the harmonics. In addition, economy in describing the fields might result if only a few harmonics are required for a good fit. To characterize the zonal average fields, we use just four amplitudes. These four amplitudes should be contrasted with the 12 monthly values for each latitude belt. We should recognize that this Fourier series is an expansion whose low-order terms involve large time scales and whose higher order terms involve shorter and shorter time scales. This is in line with our usual concept of a hierarchy of models; we expect simple models to describe the low-order harmonic terms and only the most sophisticated members of the hierarchy to describe the high-order harmonics.

We shall investigate here how well the fields may be represented in latitude by Legendre polynomials and in time by a Fourier series. The reason for using Legendre polynomials is that these functions naturally arise in the solution of certain zonally symmetric spherical boundary value problems.

Consider a zonally averaged field $F(x,t)$, where x is the sine of latitude and t is time. We seek a representation of the form

$$F(x,t) = \sum_{\substack{l=0 \\ k=0}} (a_{lk} \cos 2\pi kt + b_{lk} \sin 2\pi kt) P_l(x). \quad (1)$$

The coefficients a_{lk} and b_{lk} are to be found from least-squares fitting to observations. This is equivalent to computing the Fourier coefficients by the standard integral formulas.

There are various ways of analyzing the data—each having its own advantages and associated insights. First we use data from both hemispheres—this analysis will lead to global (G) amplitudes a_{lk}, b_{lk}. Second, we gain valuable insight by reducing the data in such a way that the asymmetry of the hemispheres is ignored. We accomplish this reduction by symmetrizing the data from one hemisphere only. For example, in the case of the Northern Hemisphere we use

$$F(-x, t) = F(x, t + \tfrac{1}{2}), \quad x > 0. \quad (2)$$

Data from the Northern Hemisphere for a particular month are used for the Southern Hemisphere, but for a period six months later. The coefficients a_{lk}, b_{lk} computed in this way will be referred to as "symmetrized northern" (SN). The symmetry condition (2) forces many of the coefficients to vanish, e.g., $a_{lk}, b_{lk} = 0$ if l is odd (or even) and k is even (or odd). We define "symmetrized southern" (SS) amplitudes in a similar manner.

The rms error $\epsilon_{L,K}$ is a measure of the error incurred in truncating the series (1) at $l = L$ and $k = K$. It is obtained from

$$\epsilon^2_{L,K} = \tfrac{1}{2} \int_{-1}^{1} dx \int_{0}^{1} dt [F_{L,K}(x,t) - F(x,t)]^2, \quad (3)$$

where $F_{L,K}$ is the subsum of (1) up to and including the $l = L$, $k = K$ terms. Note that $\epsilon_{0,0}$ is the rms deviation of the field from its global average mean annual value.

The amplitudes for several fields are presented in Tables 1–4, and the fits obtained with $L = 2$ and $k = 1$ are illustrated in Figs. 1–4 for SN. As is evident from the figures, by truncating the series at $L = 2$ and $K = 1$, we capture the hemispheric and seasonal structure of the fields. We fail to represent, however, smaller scale features. In particular, for some of the fields, we fail to accommodate the latitudinal structure in the tropics. On the other hand, owing to its simplicity the energy balance model described here is probably unable to recover this detail. In fact, in a later section we demonstrate that the model used to calculate the meridional transport of energy is inadequate for modes with $l > 2$. For these reasons we limit our examination of how well the fields are represented to the representations obtained with the series truncated at $L = 2$ and $K = 1$.

In the following discussion, $t = 0$ at 22 December, the Northern Hemisphere's winter solstice. The phase of the first harmonic ($k = 1$) is given in days; it refers to the lag between the minimum of this particular field and the minimum of the incident solar radiation. The following paragraphs describe some features of these decompositions.

a. Temperature

Table 1 shows amplitudes for the global (G), symmetrized northern (SN), and symmetrized southern (SS) 1000 mb temperature fields. For the Northern Hemisphere, the temperatures are taken from Crutcher and Meserve (1970), while for the Southern Hemisphere they are taken from Taljaard *et al.* (1969). The coefficient $a_{00} = 14.2$°C in Table 1a is the annual mean global average temperature. The coefficients a_{01}, b_{01} are an annual oscillation in the global temperature which has an amplitude 2.0°C and its maximum occurs 26.3 days after the northern summer solstice. Paradoxically, the maximum occurs just after the earth reaches its aphelion, about two weeks after the Northern Hemisphere's summer solstice. Coefficients a_{10} and a_{30} represent the mean annual asymmetry between the hemispheres since the functions $P_l(x)$ for l odd are odd functions of latitude. Coefficients a_{11} and b_{11} represent the bulk of the seasonal response in the temperature field. Coefficient a_{20} is a rough measure of the mean annual pole-to-equator temperature difference. Truncating the series at $L = 2$ and $K = 1$ leads to a 5°C rms error in the global case.

TABLE 1. Fourier-Legendre modes for 1000 mb temperatures. Phases are defined as follows: $T_{k=1}(t) = A\cos\omega(t+\phi)$ and $T_{k=2}(t) = A\cos 2\omega(t+\phi)$, where $A < 0$ and $t = 0$ at the winter solstice.

l	k	a_{lk}	b_{lk}	Amplitude	Phase (days)	rms error ϵ_{LK}
		a. Modes for global surface temperature (°C)				
0	0	14.2		14.2		15.1
	1	−1.8	−0.9	−2.0	−26.3	15.1
	2	0.0	0.0	0.0	20.9	15.1
1	0	1.7		1.7		15.0
	1	−9.1	−5.8	−10.8	−32.9	14.4
	2	−0.5	0.0	−0.5	1.1	14.4
2	0	−30.2		−30.2		4.9
	1	−3.2	−2.5	−4.1	−38.6	4.7
	2	1.0	0.6	−1.1	75.1	4.7
3	0	3.2		3.2		4.5
	1	−3.4	−0.6	−3.4	−9.6	4.4
	2	−0.5	0.3	−0.6	13.4	4.4
4	0	−8.6		−8.6		3.4
	1	2.5	0.8	−2.7	165.0	3.3
	2	1.5	0.1	−1.5	88.9	3.3
		b. Modes for symmetrized Northern Hemisphere surface temperature (°C)				
0	0	14.9		14.9		14.2
	2	−0.2	0.0	−0.2	0.7	14.2
1	1	−13.2	−8.1	−15.5	−32.1	12.7
2	0	−28.0		−28.0		2.0
	2	0.3	0.8	−0.8	57.2	2.0
3	1	−3.7	−1.7	−4.0	−24.8	1.7
4	0	−3.5		−3.5		1.3
	2	1.0	0.3	−1.1	82.7	1.2
		c. Modes for symmetrized Southern Hemisphere surface temperature (°C)				
0	0	13.5		13.5		16.0
	2	0.2	0.0	−0.2	82.9	16.0
1	1	−5.1	−3.5	−6.2	−34.9	15.8
2	0	−32.4		−32.4		6.2
	2	1.6	0.4	−1.6	83.5	6.2
3	1	−3.1	0.5	−3.1	10.1	6.2
4	0	−13.6		−13.6		4.2
	2	2.0	−0.1	−2.0	−90.5	4.2

Turning to Table 1b we see that the convergence is more rapid for the SN case and from the magnitude of the rms error we see that the fit is better. For example, truncating at $L = 2$ and $K = 1$ leads to an rms error of only 2°C. This error is sufficiently small that we may write

$$T(x,t) \approx T_0 + T_1(t)P_1(x) + T_2P_2(x), \qquad (4)$$

where $T_0 = a_{00}$, $T_2 = a_{20}$, and $T_1(t)$ is a sine function with amplitude 15.5°C and lags the incident solar radiation by 32.1 days.

The amplitudes for SS are shown in Table 1c. The amplitude of the seasonal mode is 6.2°C and the phase lag is 34.9 days. Note that the convergence and the fit are much poorer for SS.

The earth is obviously asymmetric in its seasonal response. The seasonal amplitude for SN is twice that for SS. This difference accounts for the apparent paradox in the annual harmonic a_{01} of the global mean temperature referred to above.

Fig. 1 shows seasonally averaged temperatures and the fit obtained by using (4) for SN.

b. *Infrared flux*

Table 2 shows G, SN and SS amplitudes for the infrared flux obtained from satellite observations (Ellis and Vonder Haar, 1976). We note that the $l = 1$ (seasonal) amplitude is nearly in phase with the temperature. This relationship holds especially well for the SN. It suggests that for modeling the infrared flux we might use

$$I(x,t) = A + BT(x,t). \qquad (5)$$

By applying a least squares fit of (5) to the 00, 11 and 20 modes of Tables 1b and 2b we obtain $A = 203.3$ W m^{-2} and $B = 2.09$ W m^{-2}°C^{-1}. These values for A and B apply only to the SN case. Fig. 2 shows the seasonally averaged infrared fluxes for SN and the fit obtained by using only the 00, 11 and 20 modes of Table 2b. It also shows the fit obtained with (5).

The form of (5) was suggested by Budyko (1969), and it was examined recently by Cess (1976). Cess allowed for an additional term which was proportional to the latitude-dependent cloud-cover fraction. With the additional term, he found $B = 1.6$ W m^{-2}°C^{-1}. Without the additional term, Cess would have obtained a larger value for B. The neglect of cloud cover therefore partially accounts for the difference in the two values obtained for B. We note, however, that the value derived by using our procedure contains contributions from seasonal changes in cloud cover. Considering the difference between our value and Cess's value for B, we suspect that, had we explicitly allowed for such seasonal changes in cloud cover, the resulting value of B would not have differed greatly from that given above.

c. *Albedo*

Table 3 shows amplitudes of the observed albedo in percent (Ellis and Vonder Haar, 1976). The phases are for the co-albedo (co-albedo = 1 − albedo). Fig. 3 shows the seasonally averaged albedo for SN along with the fit obtained by using the 00, 11 and 20 modes of Table 3b.

Note that for the SN the $l = 1$ amplitude of the co-albedo is in phase with the temperature. This phase relationship suggests a direct correlation between albedo and surface temperature. Two pos-

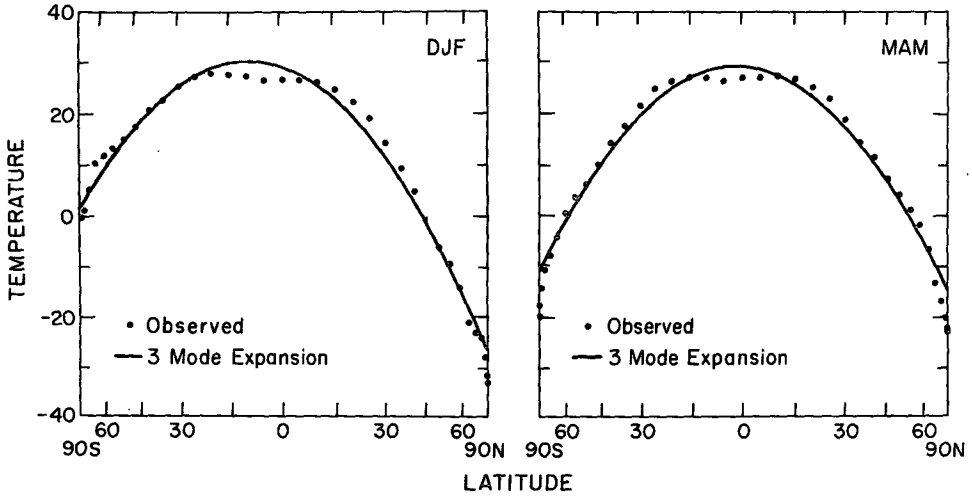

FIG. 1. Observed surface temperature of the symmetrized Northern Hemisphere (dots) and the representation of the surface temperatures obtained with the 00, 11 and 20 modes listed in Table 1b (solid curves). The surface temperatures are for Northern Hemisphere winter and spring but because the temperature fields have been symmetrized, the temperatures for summer and fall are obtained by reversing the abscissas.

sibilities for this correlation are a snow line which follows an isotherm and a cloud band which is more or less attached to an isotherm. It seems unlikely that the seasonal variation in albedo is dominated by zenith angle effects (Lian and Cess, 1977). If it were so dominated, then we would expect zero phase lag.

The $l = 1$ amplitude for the SS is only 3.6% compared to 9% for the SN. The small amplitude is consistent with the absence of land masses in the Southern Hemisphere where snow might accumulate.

For our purposes the co-albedo may be written

$$a(x,t) = a_0 + a_1(t)P_1(x) + a_2P_2(x), \qquad (6)$$

where, from Table 3b for the SN, $a_0 = 68.1\%$, a_1 is a sine wave of amplitude 9.0% and phase lag of 37.8 days behind the solar illumination, and $a_2 = -20.2\%$.

3. Incident solar radiation

In this section we discuss the Fourier-Legendre expansion for the sunlight reaching the top of the atmosphere. The form of the expansion is that of (1) with $F(x,t) = S(x,t)$, the fraction of the incident solar flux received by latitude x at time t and normalized so that the mean annual fraction integrated over the hemisphere is unity. This convention agrees with earlier work on mean annual models (Chýlek and Coakley, 1974; North, 1975a,b). To obtain the solar radiation absorbed, $S(x,t)$ must be multiplied by $Qa(x,t)$, where Q is the solar constant divided by 4 and $a(x,t)$ is the coalbedo.

We devote this section to an analysis of the mode amplitudes of $S(x,t)$. This analysis will prove useful in our discussion of the response of the model to orbital changes in Section 9.

The daily mean incident solar radiation received by latitude θ is given by Sellers (1965) as

$$S(x,\delta) = \frac{4\sigma}{\pi}[(1-x^2)^{1/2}\cos\delta\sin H + x\sin\delta H], \qquad (7)$$

where

$$\cos H = -x\tan\delta/(1-x^2)^{1/2},\ 0 \leq H \leq \pi, \qquad (8)$$

$$\sigma = \sigma_0/R^2.$$

Here δ is the solar declination, σ_0 a constant, R the earth-sun distance and, as in the previous section, $x = \sin\theta$.

The declination angle δ changes as the earth goes around the sun. From geometry we obtain

$$\sin\delta(t) = -\sin\delta_0\cos\lambda, \qquad (9)$$

where δ_0 is the obliquity and λ the longitude of the earth in its orbit. We have chosen to set $\lambda = 0$ at the Northern Hemisphere's winter solstice.

We consider the expansion of $S(x,\delta)$ into a series of $P_n(x)$. If we separate $S(x,\delta)$ into its odd and even parts, we find that the odd parts drive the seasons. If we define $W = H - \pi/2$ and insert it into (8), we obtain

$$\sin W = \frac{x}{(1-x^2)^{1/2}}\tan\delta(t), \quad -\frac{\pi}{2} \leq W \leq \frac{\pi}{2}. \qquad (10)$$

From (10) we see that W is an odd function of x. Substituting the definition of W into (7) and using (9), we also see that only one term is an odd function of x; it is given by

TABLE 2. Fourier-Legendre modes for emitted IR flux. Phases defined in caption to Table 1.

l	k	a_{lk}	b_{lk}	Amplitude	Phase (days)	rms error ϵ_{LK}
		a. Modes for global IR *flux* (W m^{-2})				
0	0	236.0		236.0		32.2
	1	−4.9	−3.3	−5.9	−34.9	31.9
	2	0.6	−2.0	−2.1	−53.4	31.9
1	0	−0.5		−0.5		31.8
	1	−26.0	−13.0	−29.0	−26.9	29.5
	2	−1.1	1.5	−1.9	64.9	29.5
2	0	−61.7		−61.7		11.1
	1	0.1	1.8	−1.8	94.6	11.1
	2	4.7	−0.2	−4.7	−90.2	11.0
3	0	7.6		7.6		10.6
	1	−13.5	−8.7	−16.1	−33.1	9.7
	2	−0.3	3.8	−3.8	43.3	9.7
4	0	−14.8		−14.8		8.3
	1	6.2	5.4	−8.2	140.8	8.1
	2	4.4	−1.8	−4.7	−79.9	8.0
		b. Modes for symmetrized Northern Hemisphere IR *flux* (W m^{-2})				
0	0	234.4		234.4		30.9
	2	−0.1	−1.7	−1.7	−44.6	30.9
1	1	−33.7	−17.7	−38.0	−28.1	26.7
2	0	−55.6		−55.6		9.5
	2	4.1	2.9	−5.0	72.9	9.3
3	1	−6.0	−1.4	−6.2	−13.7	9.2
4	0	−11.4		−11.4		8.3
	2	3.4	0.7	−3.5	84.3	8.2
		c. Modes for symmetrized Southern Hemisphere IR *flux* (W m^{-2})				
0	0	237.6		237.6		33.4
	2	1.2	−2.4	−2.6	−59.4	33.4
1	1	−18.3	−8.3	−20.1	−24.7	32.3
2	0	−66.6		−66.6		12.4
	2	5.2	−3.2	−6.1	−75.2	12.2
3	1	−21.1	−15.9	−26.4	−37.5	10.0
4	0	−18.3		−18.3		7.9
	2	5.3	−4.4	−6.9	−71.3	7.7

$$S_{\text{odd}} = -2\sigma x \sin\delta_0 \cos\lambda. \quad (11)$$

The form of (11) shows that, except for $l = 1$, all odd l coefficients in the expansion (1) vanish. Furthermore, for a circular orbit, this coefficient has only a first harmonic contribution. For elliptical orbits time-dependent corrections to λ and σ will contribute to higher harmonics.

The mode amplitudes of $S(x,t)$ are listed in Table 4. These amplitudes were computed for the present orbit. As will be demonstrated in Section 9, the $k = 0$ mode amplitudes and, to first order in the eccentricity, the a_{11} mode amplitude are independent of the eccentricity and the longitude of the perihelion. The amplitudes given in Table 4 for these modes therefore also apply to circular orbits.

For modeling purposes we may write

$$S(x,t) \approx 1 + S_1 \cos 2\pi t P_1(x) + (S_2 + S_{22} \cos 4\pi t) P_2(x), \quad (12)$$

where $S_1 = -0.796$, $S_2 = -0.477$ and $S_{22} = 0.147$. The coefficient S_{22} has a simple physical interpretation. This term is nonzero at the equator and has a semi-annual oscillation; it represents the passage of the sun twice each year over the equator. One might expect such a heating term to excite even l, semi-annual responses in the climate, but such effects are probably too small to be accounted for by the models discussed in this paper. For this reason S_{22} will be neglected in this paper.

Fig. 4 shows the seasonally averaged incident solar radiation along with the fit obtained by using the 00, 11 and 20 modes of Table 4.

4. Seasonal model

In this section we derive a seasonal model in which there is a minimum of complexity. From the derivation of the model and simple computations with it one gains insight into the features which govern the large-scale seasonal response.

We consider the seasonal energy balance equation given by

$$C(x,\phi)\frac{\partial T}{\partial t}(x,\phi,t) - D_0\nabla^2 T(x,\phi,t) + A + BT(x,\phi,t) = QS(x,t)a(x,t). \quad (13)$$

This equation includes longitude dependence. As in Fig. 5, we imagine a planet which has one continent whose borders are along meridians. For the SN we might imagine that this continent occupies 40% of the area in any latitude belt. The explicit treatment of a continent and an ocean is necessary because of the contrast between $C(x,\phi)$ over land and over water. This "thermal inertia" is an effective heat capacity per unit area. Over land we may estimate it from the heat capacity of a column of air, whereas over ocean we must also include the mixed layer which is variable in depth but may be taken here as 75 m. In the models to follow we take the thermal response over land to be the heat capacity of an atmospheric column divided by the radiation constant, $C_L/B = 0.16$ year. Likewise, over water we take the thermal response to be the heat capacity of the mixed layer divided by the radiation constant, $C_W/B = 4.7$ years. Note that these are the radiative relaxation times for the land and ocean areas in the model.

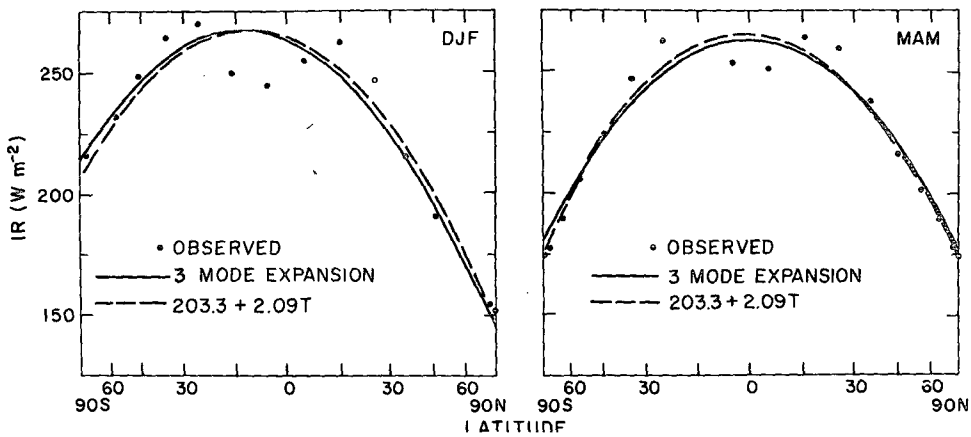

FIG. 2. Observed infrared fluxes emitted by symmetrized Northern Hemisphere (dots) and the representation obtained with 00, 11 and 20 modes listed in Table 2b (solid curves). The dashed curve shows the fit obtained by using the 00, 11, and 20 modes of the temperature field (Table 1b) in (5).

The second term in (13) represents the transport of energy and is taken to be diffusive as in the annual mean models (North, 1975a,b). The infrared terms are the same as described earlier. The absorbed heating may include temperature dependence through snow or cloud feedback, but such a dependence will be introduced in Section 8.

If we integrate (13) around a latitude belt, we obtain for the contribution from the land masses (after dividing by f_L, the fraction of land area)

$$C_L \frac{\partial T_L}{\partial t}(x,t) - D_0 \frac{\partial}{\partial x} \times (1-x^2)\frac{\partial}{\partial x} T_L - \frac{D_0}{f_L}\frac{\partial T}{\partial \phi}\bigg|_{\text{right}}^{\text{left}} + A + BT_L = QS(x,t)a_L(x,t), \quad (14)$$

where T_L is defined as the average temperature over land in the latitude belt. The third or gradient term is the difference between the land and water temperature divided by some effective angular distance over which the transition occurs. The whole term may be written

$$\frac{\nu}{f_L}(T_L - T_W), \quad \nu > 0, \quad (15)$$

where ν is a new adjustable parameter which accounts for the land-sea interaction.

Repeating this procedure for the ocean, we obtain two coupled equations given by

$$C_L \frac{\partial T_L}{\partial t} - D_0 \frac{\partial}{\partial x}(1-x^2)\frac{\partial}{\partial x} T_L + \frac{\nu}{f_L}(T_L - T_W) + A + BT_L = QS(x,t)a_L(x,t) \quad (16)$$

and

$$C_W \frac{\partial T_W}{\partial t} - D_0 \frac{\partial}{\partial x}(1-x^2)\frac{\partial}{\partial x} T_L + \frac{\nu}{f_W}(T_W - T_L) + A + BT_W = QS(x,t)a_W(x,t). \quad (17)$$

In (16) and (17) a distinction has been made between $a(x,t)$ over land and over ocean, but in most of what follows this distinction will be ignored. In the above formalism we have assumed, for simplicity, that T_L and T_W are functions only of latitude and time. The zonally averaged temperature is given by

$$T(x,t) = f_L T_L + f_W T_W, \quad (18)$$

where, as is shown in Fig. 5, f_L and f_W are independent of latitude.

One may now substitute simple truncated Legendre expansions such as (4) for both $T_L(x,t)$ and $T_W(x,t)$. Taking $a_L(x,t) = a_W(x,t)$, we obtain

$$A + BT_0 = QH_0, \quad (19)$$

$$C_{L,W}\frac{dT_1^{L,W}}{dt} + (2D_0 + B)T_1^{L,W} + \frac{\nu}{f_{L,W}}(T_1^{L,W} - T_1^{W,L}) = QH_1, \quad (20)$$

$$(6D_0 + B)T_2 = QH_2, \quad (21)$$

where

$$H_0(t) = \tfrac{1}{2}[2a_0 + a_1(t)S_1(t)G_{011} + a_2S_2G_{022} + \ldots], \quad (22)$$

$$H_1(t) = \tfrac{3}{2}[a_0S_1(t)G_{101} + a_1(t)G_{110} + a_2S_1(t)G_{121} + a_1(t)S_2G_{112} + \ldots], \quad (23)$$

TABLE 3. Fourier-Legendre modes for albedo. Amplitude and phase are for the co-albedo. The phase is defined in the caption to Table 1.

l	k	a_{lk}	b_{lk}	Amplitude	Phase (days)	rms error ϵ_{LK}
		a. Modes for global albedo (percent)				
0	0	32.0		68.0		11.3
	1	1.4	2.0	−2.4	−55.2	11.1
	2	1.4	−0.7	−1.6	14.1	11.1
1	0	−1.0		4.0		11.1
	1	5.0	1.7	−5.3	−18.8	10.8
	2	0.2	0.7	−0.8	−36.1	10.8
2	0	23.1		−23.1		3.3
	1	−0.3	1.7	1.7	82.1	3.2
	2	0.9	−1.5	−1.7	29.0	3.2
3	0	−3.6		3.6		2.8
	1	0.8	0.8	−1.1	−47.3	2.8
	2	−0.7	−1.1	−1.4	62.1	2.8
4	0	5.8		−5.8		2.0
	1	−1.1	−2.3	−2.6	117.3	1.9
	2	−1.2	−1.2	−1.7	69.4	1.9
		b. Modes for symmetrized Northern Hemisphere albedo (percent)				
0	0	31.9		68.1		10.2
	2	1.6	−0.3	−1.7	4.6	10.1
1	1	7.2	5.4	−9.0	−37.8	9.4
2	0	20.2		−20.2		2.6
	2	0.5	−1.5	−1.6	34.8	2.5
3	1	−1.3	−0.5	−1.4	161.3	2.5
4	0	3.7		−3.7		2.1
	2	−1.4	−2.8	−3.2	58.3	2.0
		c. Modes for symmetrized Southern Hemisphere albedo (percent)				
0	0	32.0		68.0		12.3
	2	1.1	−1.2	−1.6	23.0	12.2
1	1	2.9	−2.0	−3.6	35.3	12.1
2	0	26.0		−26.0		3.5
	2	1.4	−1.4	−2.0	23.7	3.4
3	1	2.8	2.1	−3.5	−37.5	3.3
4	0	7.9		−7.9		1.9
	2	−1.1	0.5	−1.2	−78.9	1.9

$$H_2(t) = \tfrac{5}{2}[a_2G_{220} + a_0S_2G_{202} + a_2S_2G_{222} + a_1(t)S_1(t)G_{211} + \ldots], \quad (24)$$

$$G_{ijk} = \int_{-1}^{1} P_i(x)P_j(x)P_k(x)dx. \quad (25)$$

The coupling coefficients G_{ijk} are $G_{011} = \frac{2}{3}$, $G_{022} = \frac{2}{5}$, $G_{121} = \frac{4}{15}$ and $G_{222} = \frac{4}{35}$. In modeling calculations it is sufficient to replace products such as $a_1(t)S_1(t)$ by their annual average and to ignore second harmonic contributions [consistent with the neglect of S_{22} in (12)]. We then see that only $H_1(t)$ has a time dependence and it is sinusoidal. The products $a_1(t)S_1(t)$ in (22) and (24) generate seasonal contributions (residuals) to the mean annual climate.

We note that (19) and (21) are identical to the equations obtained for the annual model (North, 1975b). Because of the residual $a_1(t)S_1(t)$, however, H_0 and H_2 in the seasonal model will differ from those in the annual model. The magnitude of these residuals will be estimated later. The only other new feature of the seasonal model is the seasonal amplitude equation (20).

Before exploring the solutions of the seasonal climate model (19)–(21), we reconsider the assumptions and simplifications that have made it possible. The most important assumption is that of the simple continent with latitude-independent borders. Clearly, this could have been avoided by taking $C(x,\phi)$ in (13) to be a given function over the globe and solving (13) numerically or possibly by introducing a spherical harmonic basis set. This procedure would also eliminate the need for symmetrizing the data from each hemisphere. An intermediate procedure would allow f_L and f_W to be functions of x—which complicates the mode analysis of the coupling term (15) (Sellers, 1973). Other simplifications include taking the same value of D_0 and $a(x,t)$ over land and ocean; these are undoubtedly compensated by using a lower value of ν in the coupling term.

Of course, as mentioned earlier, the diffusion hypothesis is a gross simplification. Note that for the observed albedos (Table 3b) we can use (21) and (24) to adjust D_0 so that the model gives the observed value for T_2 (a_{20} in Table 1b). If we now use the resulting value of D_0 to calculate T_4, we find that the calculated amplitude is almost an order of magnitude too small (−0.5°C compared with the observed amplitude −3.5°C in Table 1b). The failure of the model at this scale is probably due to its simple diffusive transport parameterization. Lindzen and Farrell (1977) suggest that such transport is improper in the tropics. Indeed, forcing T_4 to agree with observations by allowing D_0 to have a parabolic x dependence requires a $D_0(x)$ which is large in the tropics and small near the pole—in agreement with Lindzen and Farrell. In any case the assumption of constant D_0 seems to be invalid for scales represented by values of $n \geq 2$. Before proceeding to a more sophisticated analysis, however, we must recognize that the resulting zonally averaged seasonal temperature field requires only a few parameters for its description and that every new mechanism introduced will carry more parameters that can be subjectively tuned under a numerical smoke screen. We note also that the numerical integration of (13) also introduces the complication of waiting for transient effects to die out. This can be very expensive, since the relaxation time over the oceans is on the order of years, and to investigate a per-

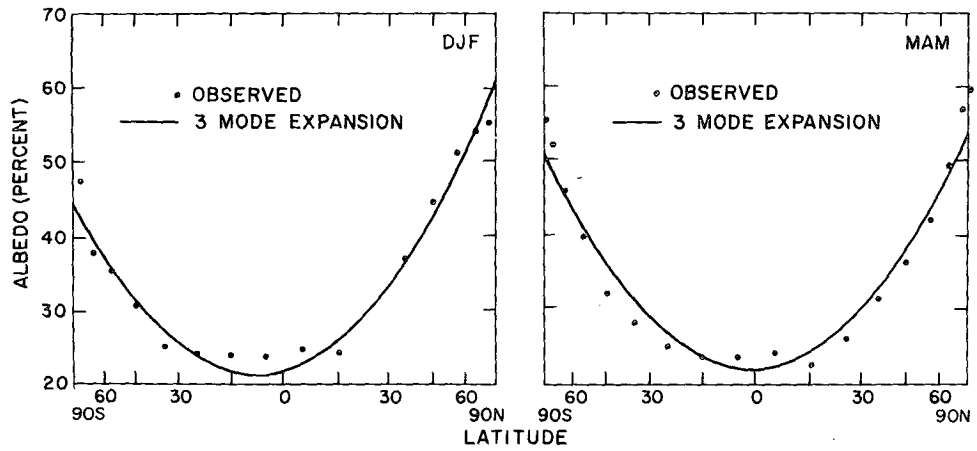

FIG. 3. Observed albedo of the symmetrized Northern Hemisphere (dots) and the representation of the albedo obtained with the 00, 11, and 20 modes listed in Table 3b (solid curves).

turbation one must wait through many e-folding times (cf. Sellers, 1973, 1974). Using (14), however, we may extract analytical "steady-state" solutions directly.

5. Present climate

This section will focus on a sequence of models for the SN which illustrate the various components that contribute to the present climate. The solutions are easily extracted from (20) by substituting sinusoidal forms for T_1^L and T_1^W and solving for the coefficients. In all cases the mean annual climate is computed from (19) and (21). For $Q = 340$ W m^{-2}, $A = 203.3$ W m^{-2}, $D = D_0/B = 0.285$, and the albedo amplitudes in Table 3b, we obtain the observed T_0 and $T_2(a_{00}$ and a_{20} of Table 1b).

a. Model 1

This is an all-land planet with no "snow" feedback [$f_L = 1, f_W = 0, a_1(t) = 0, \nu = 0$]. The value of C_L is simply adjusted to give the observed phase of $T_1(t)$. The model then predicts an amplitude of $T_1(t)$ which is 41°C to be compared with the observed value of 15.5°C (Table 1b). Alternatively, one can choose C_L so that the amplitude is correct and calculate the phase; the result is a phase lag of about 70 days—about twice the observed value. Clearly, no value of C_L is capable of giving both the amplitude and phase correctly.

b. Model 2

This is an all-land planet which includes "snow" feedback [$f_L = 1, f_W = 0, a_1(t)$ given in Table 3b, $\nu = 0$]. Again C is adjusted to give the proper phase of $T_1(t)$. In this case the model predicts an amplitude of 43°C. The snow feedback term $a_1(t) \neq 0$ intensifies the seasonal response. The snow feedback may be due to seasonal changes in cloud cover rather than to changes in snow cover. In any case the albedo change increases the seasonal amplitude.

c. Model 3

This is a planet with the continent of Fig. 5 including "snow" feedback but no land-ocean coupling [$f_L = 0.4, f_W = 0.6, C_L/B = 0.16$ years, $C_W/B = 4.7$ years, $\nu = 0$]. The model then predicts an amplitude of $T_1(t) = 19$°C with a phase lag of 41 days, to be compared with the observed 15.5°C and 32 days. Clearly, the most important effect is the large thermal inertia of the ocean. The model leads to an ocean amplitude $|T_1^W(t)|$ about 3°C with phase lag of nearly three months—the latter is character-

TABLE 4. Fourier-Legendre modes for distribution of incident solar radiation $S(x,t)$. The mode amplitudes are zero for $l = 2n + 1$, where $n > 0$. Phases are defined in the caption to Table 1.

l	k	a_{lk}	b_{lk}	Amplitude	Phase (days)	rms error ϵ_{LK}
0	0	1.000		1.000		0.393
	1	0.033	0.007	−0.034	170.1	0.393
	2	0.001	0.000	−0.001	77.4	0.393
1	0	0.000		0.000		0.393
	1	−0.796	0.006	−0.796	0.4	0.221
	2	−0.026	−0.006	−0.027	−6.1	0.221
2	0	−0.477		−0.477		0.056
	1	−0.018	−0.003	−0.018	−9.3	0.030
	2	0.147	−0.002	−0.147	−90.9	0.030
4	0	−0.045		−0.045		0.026
	1	−0.003	0.000	−0.003	−0.5	0.026
	2	0.089	−0.001	−0.089	−90.9	0.015

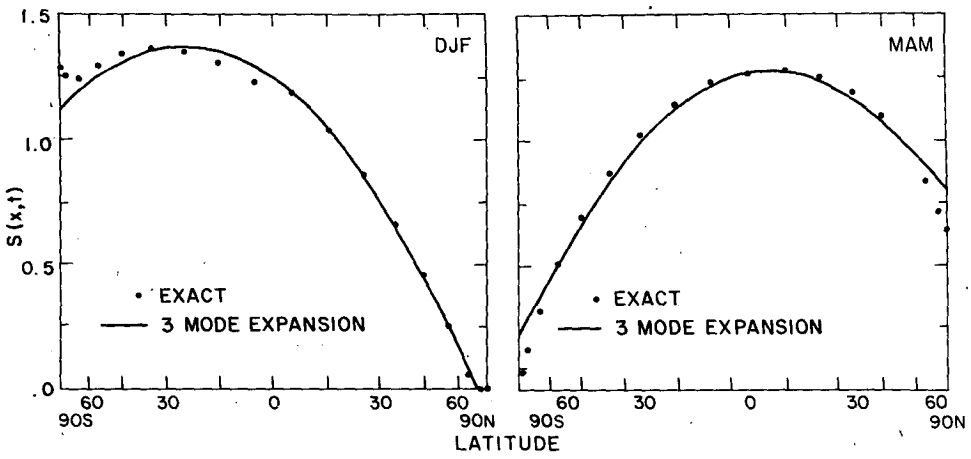

FIG. 4. Distribution of incident solar radiation (dots) and the representation of the distribution obtained with the 00, 11 and 20 modes listed in Table 4 (solid curves).

istic of an infinite C_W/B and is rather insensitive to C_W/B so long as it is greater than about one year. The amplitude of T_1^W is roughly inversely proportional to C_W and could be increased by reducing the rather arbitrarily chosen mixed-layer depth. The land temperature amplitude is about 41°C—a value that seems large.

Clearly, one can lower the amplitude of $T_1^L(t)$ by taking $\nu > 0$. By increasing ν one effectively couples the land to a large thermal reservoir. The ocean amplitude is hardly affected, while the land amplitude is reduced. A value of $\nu/B = 0.226$ brings the amplitude of T_1 to the observed value of 15.5°C, while the phase is late by about one week. The observed and calculated amplitudes and phases are listed in Table 5. Reducing C_L by about 15% and readjusting ν/B, we obtain the observed phase and amplitude. The model is sufficiently crude that including more effects seems unjustified.

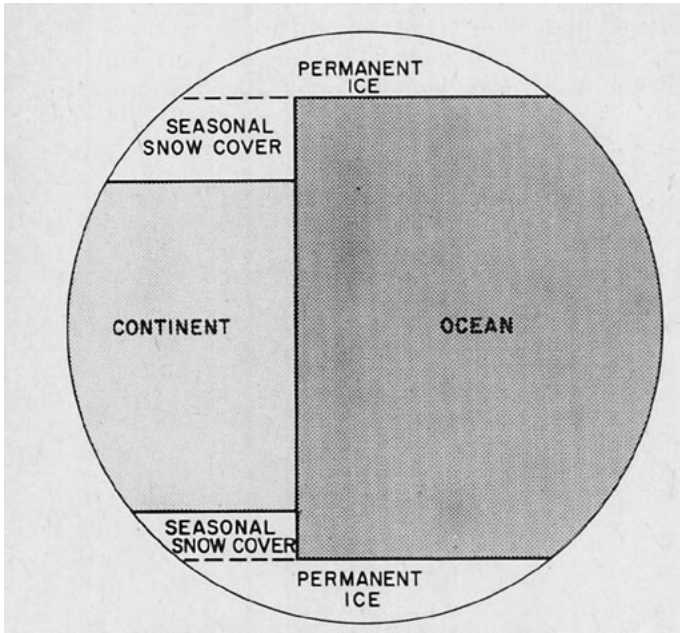

FIG. 5. Schematic showing the distributions of land, ocean, permanent ice and snow in the seasonal model.

6. Model test

While the previous section provides support for the notion that simple models can simulate the large-scale features of the climate, one has the uneasy feeling that too many parameters have been adjusted. In this section we investigate a different planet, the symmetrized Southern Hemisphere (Table 1c). For this study we use $f_L = 0.2$ and the albedo for the Southern Hemisphere (Table 3c). As is shown in Table 6, the model predicts an amplitude of 7.8°C for $T_1(t)$ with a phase lag of 40 days to be compared with the observed values of 6.2°C and 35 days. The values of T_0 and T_2 are also within 2°C of the observed values. The value obtained for T_0 becomes 12.4°C if A of the radiation formula is adjusted for the Southern Hemisphere temperature and cloud data (Cess, 1976). It seems that these results agree sufficiently to warrant use of this type of model to study climatic sensitivities.

TABLE 5. Observed and calculated mode amplitudes and phase for SN surface temperature. The amplitudes were computed for the albedo (Table 3b) and land area fraction of SN. The model parameters A, D and ν were adjusted to give the observed magnitudes of T_0, T_1 and T_2.

	Calculated	Observed
T_0	14.9	14.9
T_1	$-15.5\cos(\omega t - 37.9)$	$-15.5\cos(\omega t - 32.1)$
T_2	−28.0	−28.0

TABLE 6. Observed and calculated mode amplitudes and phase for SS surface temperature. The amplitudes were computed with the albedos (Table 3c) and the land area fraction of SS but with the model parameters, A, D and ν adjusted to give the observed magnitudes of T_0, T_1 and T_2 of SN.

	Calculated	Observed
T_0	14.8	13.5
T_1	$-7.8\cos(\omega t - 40.3)$	$-6.2\cos(\omega t - 34.9)$
T_2	-31.5	-32.4

7. Seasonal effects on the mean annual climate

One obvious use of a seasonal climate model is to estimate the errors involved in using a mean annual model. While hardly a foolproof procedure, one can nonetheless make some quantitative statements about differences between annual mean and seasonal model results. In this section we investigate the magnitude of such differences.

Differences are due to what may be termed the snow feedback effect. This effect involves the residual interaction terms proportional to $a_1(t)S_1(t)$ in the heating components H_0 and H_2 [Eqs. (22) and (24)]. From (19) and (22), the change in the average annual mean temperature is given by

$$\Delta T_0 = Q\langle a_1(t)S_1(t)\rangle G_{011}/2B, \qquad (26)$$

where the angle braces represent the annual average $-\langle a_1(t)S_1(t)\rangle = \frac{1}{2}a_1S_1\cos\phi$, where ϕ is the phase difference (38 days for the SN). The result is $\Delta T_0 = 1.5$°C for SN. The seasonal oscillation in albedo causes a warming due to the fact that the hemisphere is snow free in summer and therefore absorbs well, while in winter when snow advances, the polar cap is tilted away from the sun so that its high reflectivity matters less. We therefore have a warmer hemisphere than might have been obtained with a mean annual snow line. Of course, within the framework of this simple model, the same applies if the time dependence in $a_1(t)$ is due to cloud movements. It is important to note that (26) does not assume any model for $a_1(t)$. A similar warming effect was observed in GCM results obtained by Wetherald and Manabe (1972).

The cross term $a_1(t)S_1(t)$ also appears in H_2 [Eq. (24)] leading to a change in T_2 which may be estimated from (21):

$$\Delta T_2 = \tfrac{5}{2}Q\langle a_1(t)S_1(t)\rangle G_{211}/(6D_0 + B), \qquad (27)$$

which has a magnitude of about 1.1° for the SN, compared to $T_2 = -28.0$°C. The mean annual equator-to-pole temperature difference in the two-mode approximation is $-\frac{3}{2}T_2$ so the term (27) reduces this difference by about 1.6°C. The combined effects of (26) and (27) lead to a pole warmer by 2.6°C and an equator warmer by 1.0°C. The results of these calculations are compared with those obtained with a GCM (Wetherald and Manabe, 1972) in Fig. 6.

The estimates made above are merely meant to be illustrative of the order of magnitude of seasonal residuals on the mean annual climate. There are surely other residuals. For example, one might expect a seasonal part of D_0 to interact with T_1, or a change in the mixed layer depth and thus in C_W to interact with T_1. Without a physical model for such interactions, however, estimates of the corresponding residuals could be subject to large uncertainties.

8. Sensitivity to changes in solar constant

In the previous sections, a model was developed which was capable of simulating the large-scale features of the zonally averaged seasonal cycle. In this section and the next section we use the model to study departures from the present climate. These results will be compared with those of the corresponding mean annual model. In studying climate change, however, a set of time scales may be involved which differ from those important in the seasonal oscillation. As a result, feedback mechanisms so far not considered may become active. In any case the set of assumptions must be augmented.

For our study we choose to alter only the temperature-albedo feedback. We allow for a seasonally varying snow line on land and for an ice cap whose

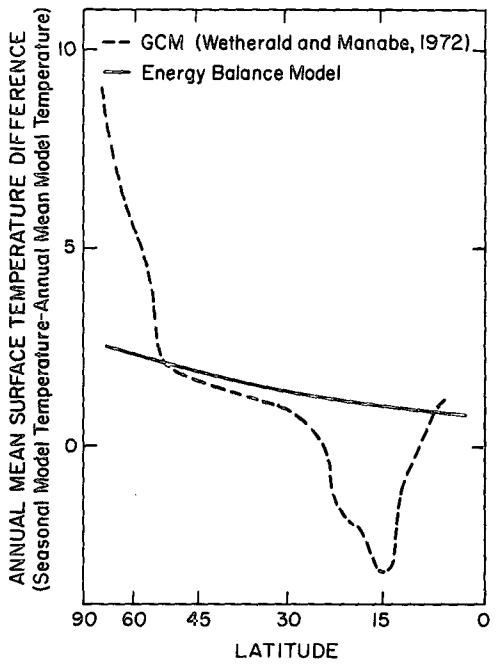

FIG. 6. Differences between annual mean surface temperatures computed with seasonal and annual mean models.

TABLE 7. Amplitudes for the absorbed flux of solar radiation calculated with the seasonal model and taken from satellite observations analyzed by Ellis and Vonder Haar (1976). Amplitudes are in W m^{-2} and phases are in number of days from the Northern Hemisphere's winter solstice.

	Observed	Calculated
QH_0	241	236
QH_1	$-181\cos(\omega t - 5.9)$	$-193\cos(\omega t - 1.5)$
QH_2	−161	−143

area is determined by mean annual conditions. With these features the model becomes nonlinear. To obtain exact solutions it is therefore necessary to use an iterative method. However, we shall continue to use the truncated spectral approach so that the dependent variables are the first few mode amplitudes of the temperature field. As before, this procedure eliminates the transient effects and extracts the steady-state periodic solutions. The procedure, of course, acts as a filter, removing small-scale information in space and time. That the small-scale structure has little influence on the large-scale structure must be thought of as an essential assumption in the present model.

To compute the albedo-temperature feedback the following model is used for the albedo. A permanent ice line is located at the −10°C isotherm of the zonal average annual mean temperature. Ice cover poleward of the ice line is common to both land and ocean areas in the model. The ice line remains fixed throughout the annual cycle. On land, snow cover extends to the 0°C isotherm of the land surface temperature and, in this way, seasonal changes in the snow cover of the continents is modeled. Seasonal changes in the position of the ice line are not allowed in the model. Surface albedos and zenith-angle-dependent reflectivities for the ocean surface and for clear skies are obtained from the parameterizations described by Coakley (1979). The zenith-angle-dependent reflectivity of cloudy skies is taken from Lian and Cess (1977). The cloud cover fraction is set to be constant at 50% for all latitudes and over both land and ocean areas. With the parameters of the seasonal model adjusted to give the observed temperatures, as is described next, this simple model for the albedo yields results which agree well with observations. The calculated and observed amplitudes of the low-order modes for the absorbed solar radiative flux are listed in Table 7.

The sensitivity of energy balance models depends on the values used for the model parameters, and the parameters of both the seasonal model and its corresponding annual mean model in this study were adjusted so that both models produced the observed amplitudes of the mean annual temperature modes. In the seasonal model, A, D_0 and ν were adjusted to give $T_0 = 14.9$°C, $|T_1| = 15.5$°C and $T_2 = -28.0$°C, as given in Table 1b. These amplitudes were obtained when $Q = 340$ W m^{-2}, $A = 204.6$ W m^{-2}, $D_0/B = 0.238$ and $\nu/B = 0.387$. Because the land and ocean areas have different albedos in this version of the model, a value of ν larger than that used earlier ($\nu/B = 0.226$) was required to obtain the observed T_1. In this version the depth of the ocean mixed layer was also reduced from 75 to 50 m in order to simulate more closely the amplitude of the seasonal surface temperature change over oceans. With the reduced mixed layer depth, this amplitude was about 6°C.

The parameters of the corresponding annual mean model were adjusted to give the observed T_0 and T_2. The resulting constants were $A = 202$ W m^{-2} and $D_0/B = 0.264$. These constants differ from those for the seasonal model because the snow line and incident solar radiation change with time in the seasonal model, whereas they are fixed at their mean annual levels in the annual mean model. For the same latitudinal distribution of annual mean temperatures, these differences cause the two models to compute different fluxes of absorbed solar radiation. The difference between constants reflects the difference between the radiation budget components of the two models.

The change in T_0 for a 1% decrease in Q was found to be −1.67°C for the seasonal model and −1.63°C for the annual mean model. Thus, the two models exhibit essentially the same sensitivity.

The temperature change obtained with both models was much smaller than the −4 to −5°C changes obtained by Budyko (1969), Sellers (1969) and North (1975b) using earlier annual mean models. As was shown by Lian and Cess (1977) and by Coakley (1979), this difference in sensitivities is caused primarily by differences in the albedo parameterizations and to a lesser extent by differences in B.

Often solutions for simple energy balance models are displayed in terms of the position of the permanent ice line as a function of the solar constant. Fig. 7 shows the ice-line position for both annual mean and seasonal models. The solution to the seasonal model jumps to an ice-covered earth solution when $Q/Q_0 = 0.89$, where Q_0 is the present solar constant, and that for the annual mean model jumps for $Q/Q_0 = 0.91$. As the figure shows, the two models behave nearly identically for changes in the solar constant.

9. Sensitivity to changes in orbital parameters

Milankovitch argued that changes in the incident solar radiation caused by changes in the earth's orbit forced the periodic glaciation of the earth. So far, however, attempts to support this hypothesis with simple annual mean energy balance models have

failed (Coakley, 1979). Whereas the ice-line reached 60°N during the 18 000 YBP glacial maximum, a latitude difference of almost 15° from the present ice-line, annual mean models produced advances of only 2–4° for the change in obliquity thought to be responsible for the glaciation. On the other hand, Budyko (1969) noted that changes in the orbital parameters caused only small changes in the latitudinal distribution of the annual mean incident solar radiation and that seasonal changes could be two to three times as large. In this section we use the truncated model described in the last section to check this hypothesis.

Past changes in the eccentricity e, the longitude of the perihelion relative to the winter solstice Π, and the obliquity δ_0, can affect the distribution of solar radiation reaching the earth, $S(x,t)$. In keeping with the class of models discussed in this paper, we shall only investigate effects on the mean annual and first harmonic in time and on the $n = 0, 1, 2$ Legendre polynomial mode amplitudes of $S(x,t)$. These will in turn force changes in the lowest modes of the temperature field.

If the orbital changes are due to the perturbations of other planets, the overall solar constant changes by a factor of approximately $(1 + \frac{1}{2}\Delta e^2)$, where Δe^2 is the change from the present value (Vernekar, 1971; Berger, 1978). We see that as e varies from 0 to 0.06, the effective solar constant varies by less than 0.4%. This effect may then be dismissed in the present class of models since it would lead to changes in T_0 of only 0.7°C. In the last 25 000 years the change in e was less than 0.001, which would cause a change in T_0 of about 0.02°C for the present parameterization of the mean annual model.

With regard to the mode amplitudes of $S(x,t)$ we consider the seasonal forcing $S_1(t)$ which was computed analytically in Section 3 [Eq. (11)]. We shall show that to first order in the eccentricity a_{11} in Table 4 is independent of both e and Π. The first harmonic amplitudes are given by the standard formula for Fourier coefficients

$$\begin{pmatrix} a_{11} \\ b_{11} \end{pmatrix} = -\int_0^1 dt 4\sigma x \sin\delta_0 \cos\lambda \begin{pmatrix} \cos 2\pi t \\ \sin 2\pi t \end{pmatrix}, \quad (28)$$

where

$$\sigma = \sigma_0[1 + e\cos(\lambda - \Pi)]^2/r_0^2, \quad (29)$$

with constants σ_0 and r_0. Both λ and t are zero at northern winter solstice. It is convenient to change variables in (29) from time t to longitude λ. From conservation of angular momentum we obtain

$$\frac{mr_0^2}{(1 + e\cos(\lambda - \Pi))^2}\frac{d\lambda}{dt} = \text{constant}. \quad (30)$$

Thus,

$$\begin{pmatrix} a_{11} \\ b_{11} \end{pmatrix} = -Qx \sin\delta_0 \int_0^{2\pi} d\lambda \cos\lambda \begin{pmatrix} \cos 2\pi t(\lambda) \\ \sin 2\pi t(\lambda) \end{pmatrix}, \quad (31)$$

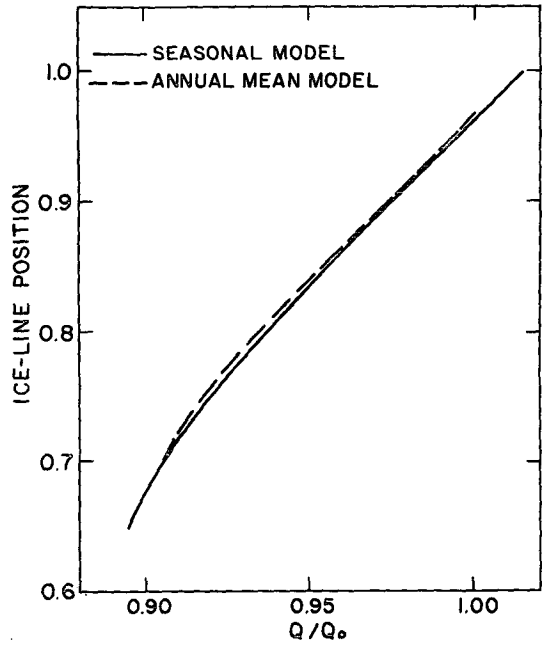

FIG. 7. Sine of latitude of permanent ice line (−10°C isotherm of annual mean temperature field) as a function of incident solar radiative flux Q for seasonal model (solid curve) and for annual mean model (dashed curve). Q_0 is the solar constant.

where Q is a constant. Eq. (30) may be integrated to obtain the relationship between λ and t. The result may be written as a power series in e:

$$\begin{pmatrix} \cos 2\pi t \\ \sin 2\pi t \end{pmatrix} \approx \begin{pmatrix} \cos\lambda \\ \sin\lambda \end{pmatrix} - 2e \begin{pmatrix} -\sin\lambda \\ +\cos\lambda \end{pmatrix} \times [\sin(\lambda - \Pi) - \sin\Pi] + O(e^2) \ldots . \quad (32)$$

Direct substitution of (32) into (31) shows that, to first order in e, a_{11} is independent of e and Π. These two quantities therefore do not affect the component of $S(x,t)$ which was responsible for forcing the seasons.

However, there are e-dependent, first-harmonic contributions to $S(x,t)$ which are nonvanishing. Note, for example, that $b_{11} = -a_{11}(2e\sin\Pi)$. Another first-harmonic amplitude also appears in the global average mode $S_0(t)$. It has an amplitude which is given by $2e\cos(2\pi t - \Pi)$, and it is clearly identifiable as the coefficients a_{01} and b_{01} in Table 4. A similar (order e) first harmonic term is present in $S_2(t)$. These are the only dependences on e and Π that should be considered in the present truncated model. The mode amplitudes of $S(x,t)$ do acquire higher harmonics which are proportional to higher powers of e, but we do not allow these in the model. The magnitudes of these terms are extremely small and hence the decision to omit them is justified.

The eccentricity and longitude of perihelion do not affect the mean annual components of $S(x,t)$. This

can be seen by integrating $S(x,t)$ over time before doing the latitudinal analysis. After changing to the λ variable as before, we have

$$S(x) = Q \int_0^{2\pi} d\lambda[(1 - x^2)^{1/2} \cos\delta(\lambda) \cos W(\lambda) - x \sin\delta_0 \cos\lambda W(\lambda)], \quad (33)$$

which does not depend on e or Π.

Finally, we note that the obliquity δ_0 occurs in both the seasonal forcing [as $\sin\delta_0$ in Eq. (28)] and in a more complicated way in the mean annual component S_2. The latter affects mean annual models and is the primary perturbation used by previous authors (e.g., Coakley, 1979) to estimate such responses.

We now consider how the seasonal model responds to these perturbations in the forcing. The nonlinear model of the previous section is used but, in fact, most results are easily interpreted from the discussion of seasonal residuals in Section 7. The changes due to various effects are small enough that they may be considered one at a time and the corresponding responses added.

First consider the obliquity. For a decrease in the obliquity, high latitudes receive less solar radiation and low latitudes receive more. Because of the albedo-temperature feedback at high latitudes, it would seem that low obliquity orbits would favor the development of large glaciers. Lowering the obliquity from the present 23.45° to the 25 000 YBP 22.25°, which is thought to have spurred the last glacial advance, causes S_1 and S_2 in (12) to change, $S_1 = -0.732$ and $S_2 = -0.491$. This change in the distribution of incident solar radiation moves the ice line in the seasonal model only 3° of latitude equatorward. For the same change in the annual mean model the ice line moves 2° equatorward. The larger change in the seasonal model is primarily caused by the residuals in the absorbed solar radiation [Eqs. (26) and (27)].

Now consider model responses to changes in e and Π. In a model which retains first harmonics these changes can enter, for example, the S_{01} and S_{21} modes of the heating. The largest residual we can imagine contributing to H_0 (22) leads to a change in T_0 given by

$$\Delta T_0 \approx Q \frac{|S_{01}||a_{01}|}{2B}, \quad (34)$$

where S_{01} and a_{01} are the seasonal components of the global incident radiation and co-albedo. The latter might come about if we allowed for the north–south asymmetry in the model. The cross-term $S_{01}(t)a_{01}(t)$ is not represented in (22) because in a symmetric model $a_{01} = 0$. As we have shown, $|S_{01}| \approx 2e$ (=0.03 at present) and, from Table 3, $a_{01} \approx 0.09/4$, where the denominator is obtained by assuming no albedo change in the Southern Hemisphere and area weighting the albedo over the globe. Thus, $\Delta T_0 \approx 0.06$°C. Changes in the $P_1(x)$ and $P_2(x)$ temperature modes are readily shown to be of similar magnitude. Such changes should be compared with the enhancement in the seasonal model obtained for the change in obliquity. The enhancement is obtained from (26) and is given by

$$\Delta T_0 \approx \frac{Q|\Delta S_1||a_1|}{6B}. \quad (35)$$

With $|\Delta S_1| \approx 0.06$ and $|a_1| \approx 0.09$, we obtain $\Delta T_0 \approx 0.1$°C. Thus, changes in the longitude of perihelion could cause a difference in the response of the two models, which is at most only comparable to the difference obtained above for the change in obliquity.

The responses obtained with the seasonal and annual mean models are comparable to those obtained by others (Budyko, 1969; Suarez and Held, 1976; Coakley, 1979). They are much smaller, however, than the 15° shift in latitude that occurred between the 18 000 YBP glacial maximum and the present. Since the models fall so short of explaining the glacial advances by changes in the earth's orbital elements, we are forced to look for new low-frequency feedback mechanisms.

We should remember, however, that the model studied here is admittedly simplistic. For one thing, it contains snow and ice lines which are tied to isotherms. Perhaps a more realistic approach has recently been undertaken by Pollard (1978), who combines a seasonal model similar to ours with the glacial model of Weertman (1976). Since a snow budget is retained, both the local radiative heating and the local temperature affect melting rates and thereby snow cover. This type of coupling between solar insolation and snow melt could increase the sensitivity of the model to orbital perturbations. Perhaps another improvement would be to use a model for the ocean mixed layer that is more realistic than the passive thermal reservoir model used here. By adding to his energy balance model a simple model for the mixed layer, Budyko (1974) obtained glacial-type conditions in response to past orbital changes.

10. Conclusions

The purpose of this paper has been to extend the simple mean annual Budyko-Sellers climate models to include the seasonal cycle. It was shown that observed fields (if symmetrized so that both hemispheres behave identically) could be represented by just a few terms in an expansion employing Legendre polynomials in latitude and sinusoidal harmonics in time.

Once it was established that the forcing (solar input) and responses (temperature field) were representable by such a simple truncated series, it was easy to derive the transfer matrix relating the two. The single most important control on the seasonal amplitude was the fraction of the planetary surface covered by water.

It was noted that several phase relationships were important in the reduced data fields: the temperature field lagged the solar input by about one month, while the infrared radiation emitted to space and the co-albedo were in phase with the temperature.

We showed that residuals due to the time-dependent albedo and incident solar radiation caused the global average mean annual temperature to be about 1.5°C higher in the seasonal model than in the mean annual model. The residuals also caused the pole-to-equator temperature difference to be about 1.6°C smaller.

Combining a simple parameterization of the albedo with a variable snow line attached to the 0°C isotherm on land and an ice cap edge attached to the −10°C mean annual isotherm, we solved the model numerically and examined its sensitivity with respect to changes in the solar constant. Even with the seasonally varying snow line, we found no appreciable difference in sensitivity with the corresponding mean annual model.

The model was used to check the Milankovitch hypothesis that advances of the polar ice caps are related to changes in the earth's orbital elements. After we analyzed the mode amplitudes of the solar forcing for changes due to changes in the orbital elements, we estimated the changes in the temperature mode amplitudes. The largest response was due to changes in obliquity with the responses due to changes in eccentricity and longitude of perihelion being smaller. Even so, the responses in global average temperature were a factor of 5–10 smaller than the changes thought to have occurred during the last million years. Although empirical evidence seems to be mounting that there is a Milankovitch connection (Hays *et al.*, 1976), our null results agree with previous studies of mean annual models in failing to provide a satisfactory mechanism.

However, we should caution the reader that our results are not a strict test of the Milankovitch theory, since in this study many idealizations have been made in the interest of tractibility and clarity. Furthermore, we have chosen only one type of dominant low-frequency feedback mechanism (temperature-albedo) in our study. We feel, however, that the methodology introduced here can be used as a framework for further discussion of this interesting problem.

Acknowledgment. This research was supported in part by the Climate Dynamics Program, Climate Dynamics Research Section, Atmospheric Sciences Division National Science Foundation and in part by funds from Goddard Laboratory for Atmospheric Sciences, Goddard Space Flight Center/NASA. We are especially grateful to Ms. H. R. Howard and Ms. Kimi McKinnon for diligently typing the manuscript and tables.

REFERENCES

Adem, J., 1962: On the theory of the general circulation of the atmosphere. *Tellus*, **14**, 102–115.

Berger, A. L., 1978: Long-term variations of caloric insolation resulting from the earth's orbital elements. *Quat. Res.*, **9**, 139–167.

Budyko, M. I., 1969: The effect of solar radiation variations on the climate of the earth. *Tellus*, **21**, 611–619.

Budyko, M. I., 1974: *Climate and Life*. Academic Press, 308 pp.

Cess, R. D., 1976: Climate change: An appraisal of atmospheric feedback mechanisms employing zonal climatology. *J. Atmos. Sci.*, **33**, 1831–1843.

Chýlek, P., and J. A. Coakley, Jr., 1975: Analytical analysis of a Budyko-type climate model. *J. Atmos. Sci.*, **32**, 675–679.

Coakley, J. A., Jr., 1979: A study of climate sensitivity using a simple energy balance model. *J. Atmos. Sci.*, in press.

Crutcher, H. L., and J. M. Meserve, 1970: *Selected-Level Heights, Temperatures and Dew Point Temperatures for Northern Hemisphere*. NAVAIR 50-1C-52, Washington, DC. [Available from Chief, Naval Operations].

Ellis, J., and T. H. Vonder Haar, 1976: Zonal average earth radiation budget measurements from satellites for climate studies. Atmos. Sci. Pap. 240, Colorado State University, Fort Collins, 57 pp.

Fritz, S., 1960: The heating distribution in the atmosphere and climatic change. *Dynamics of Climate*, R. L. Pfeffer, Ed., Pergamon Press, 96–100.

Hays, J. D., J. Imbrie, and N. J. Shackleton, 1976: Variations in the earth's orbit: Pacemaker of the ice ages. *Science*, **194**, 1121–1132.

Held, I. M., and M. J. Suarez, 1974: Simple albedo feedback models of the ice caps. *Tellus*, **26**, 613–629.

Kukla, G. J., 1975: Missing link between Milankovitch and climate. *Nature*, **253**, 600–603.

——, and H. J. Kukla, 1974: Increased surface albedo in the Northern Hemisphere. *Science*, **183**, 709–714.

Lian, M. S., and R. D. Cess, 1977: Energy balance climate models: A reappraisal of ice-albedo feedback. *J. Atmos. Sci.*, **34**, 1058–1062.

Lindzen, R. S., and B. Farrell, 1977: Some realistic modifications of simple climate models. *J. Atmos. Sci.*, **34**, 1487–1501.

North, G. R., 1975a: Analytical solution to a simple climate model with diffusive heat transport. *J. Atmos. Sci.*, **32**, 1301–1307.

——, 1975b: Theory of energy-balance climate models. *J. Atmos. Sci.*, **32**, 2033–2043.

Pollard, D., 1978: An investigation of the astronomical theory of the ice ages using a simple climate-ice sheet model. *Nature*, **272**, 233–235.

Saltzman, B., and A. D. Vernekar, 1971: Note on the effect of earth orbital radiation variations on climate. *J. Geophys. Res.*, **76**, 4195–4197.

Schneider, S. H., and R. E. Dickinson, 1974: Climate modeling. *Rev. Geophys. Space Phys.*, **12**, 447–493.

Sellers, W. D., 1965: *Physical Climatology*. The University of Chicago Press, 272 pp.

——, 1969: A climate model based on the energy balance of the earth-atmosphere system. *J. Appl. Meteor.*, **8**, 392–400.

——, 1970: The effect of changes in the earth's obliquity on the distribution of mean annual sea-level temperatures. *J. Appl. Meteor.*, **9**, 960–961.

——, 1973: A new global climatic model. *J. Appl. Meteor.*, **12**, 241–254.

——, 1974: A reassessment of the effect of CO_2 variations on a simple global climatic model. *J. Appl. Meteor.*, **13**, 831–833.

——, 1976: A two-dimensional global climatic model. *Mon. Wea. Rev.*, **104**, 233–248.

Suarez, M. J., and I. M. Held, 1976: Modeling climatic response to orbital parameter variations. *Nature*, **263**, 46–47.

Taljaard, J. J., H. van Loon, H. L. Crutcher, and R. L. Jenne, 1969: *Climate of the Upper Air: Southern Hemisphere*. Vol. 1, *Temperatures, Dew Points, and Heights at Selected Pressure Levels*, NAVAIR 50-1C-55, Washington, DC. [Available from Chief, Naval Operations.]

Vernekar, A. D., 1971: *Long-Period Global Variations of Incoming Solar Radiation. Meteor. Monogr.*, No. 34, Amer. Meteor. Soc., 21 pp + tables.

Weertman, J., 1976: Milankovitch solar radiation variations and ice age ice sheet sizes. *Nature*, **261**, 17–20.

Wetherald, R. T., and S. Manabe, 1972: Response of the joint ocean-atmosphere model to the seasonal variation of the solar radiation. *Mon. Wea. Rev.*, **100**, 42–58.